

The symbiotic system Z Andromedae : a spectral analysis of the anomalous 1984-1986 outburst

M. Contini

School of Physics and Astronomy, Tel-Aviv University, Tel-Aviv, 69978 Israel

Abstract

The visual magnitude profile of the symbiotic system Z And during the 1984-1986 activity period appears double peaked and the flux intensity is low compared to outbursts in other epochs. The detailed modeling of the observed spectra, accounting for the shells ejected by the red giant star, shows that the outburst is intrinsically single but distorted by the collision at different phases of the white dwarf wind with two close shells.

Keywords: binaries: symbiotic - stars: individual: Z And

1. Introduction

Symbiotic systems (SS) are generally composed by a white dwarf (WD), a red giant (RG) star, and by circumstellar and circumbinary nebulae. Gas and dust radiation from the nebulae appear throughout a large frequency range, from radio to X-rays.

Z Andromedae (Z And) binary system consists of a cool giant of spectral type M4.5 and a hot compact component with a temperature of $\sim 1.5 \cdot 10^5$ K. Many periods of activity have been reported during more than 100 years, in 1915, 1939, 1960, 1984, and 2000 as nonuniform eruptions of classical outbursts. Sokolowski et al. (2006) claim that the *outbursts sometimes come in pairs (as in 1984 and 1986)*, or in a series of eruptions with decreasing maximum brightness and different shapes, separated in time by periods slightly shorter than the orbital one (Kenyon & Webbink 1984).

The main characteristics of the 1984-1986 event are the two maxima which appear in the profile of the visual magnitude (Fernández-Castro et al. 1995, hereafter FC95, fig. 1) leading to the ambiguous interpretation of the outburst as a double or a disturbed single one. FC95 suggested, on the basis of

the line ratio analysis, that a drop in the WD radiation flux could provoke the observed trend of the light curve in 1986. They claim that a shell of material was ejected during each of the *two outbursts* at 1984 and 1986.

The brightness of the 1984-1986 event was exceptionally low (Leibowitz & Formigini 2008, fig. 1). Nevertheless, it was monitored at very close dates by the spectral observations of FC95. The spectra are rich enough in number of lines to allow a detailed modeling of Z And physical conditions.

In this paper we revisit Z And system focusing on the physical conditions in the nebulae and their fluctuations in the 1984-1986 years. Our aim is to reveal unpredicted episodes by the detailed modeling of the spectra.

In Z And, the stellar wind of the cool giant has a velocity of $\sim 25 \text{ km s}^{-1}$ (Sequist et al. 1984). Bisikalo et al (2006) claim that varying the wind velocity from 25 km s^{-1} to 30 km s^{-1} changes the accretion regime from disk to wind accretion. This is accompanied by a jump in the accretion rate, increasing the hydrogen burning rate. An optical thick wind forms from the WD. This wind is revealed e.g. by the observations of UV and optical spectra during the 2000-2002 outburst (e.g. Sokoloski et al 2006, Tomov et al 2008).

The shocks which derive from WD and RG wind collision yield an increase in the luminosity of the system. This hypothesis is strengthened by FC95 who did not find evidence for an accretion disk at the 1984-1986 epoch but suggested collision episodes.

Collision of the winds (Girard & Willson 1987, Bisikalo et al 2006, Angeloni et al 2010, Contini & Angeloni 2011) leads to two shock fronts between the stars : the strong one, dominating the spectrum, propagates in reverse towards the WD, while the weakest one propagates towards the RG. Moreover, a shock front expands out of the system throughout the circumbinary medium.

We calculate the line spectra in Sect. 2 in the frame of the wind collision model, adopting the code SUMA¹, which accounts consistently for shocks and photoionization. The input parameters are: the shock velocity V_s , the preshock density n_0 , the preshock magnetic field B_0 , the colour temperature of the hot star T_* , the ionization parameter U relative to the black body (BB) flux reaching the nebula. The geometrical thickness of the emitting nebula D , the dust-to-gas ratio d/g , and the abundances of He, C, N, O, Ne, Mg, Si, S, A, Fe relative to H are also accounted for. $B_0=10^{-3}$ gauss is

¹[//wise-obs.tau.ac.il/~marcel/suma/index.htm](http://wise-obs.tau.ac.il/~marcel/suma/index.htm)

adopted.

The observations at different epochs of the continuum spectral energy distribution (SED) are reproduced in Sect. 3 by models constrained by the fit of the line ratios. The adjustment factors determine the distance of the nebulae downstream of shock fronts from the system center, providing a detailed picture of the Z And components. Discussion and concluding remarks follow in Sect. 4.

2. Line spectra

The trend of the spectral observations between 1978 and 1993 (FC95, figs. 4,5) gives a first hint about the 1984-1986 outburst in the frame of a longer activity period. We notice that :

- 1) the 1984-1986 outburst lies upon an event which developed about at 1979 and ended at 1988. If this long event depends on the WD activity, then the temperature of the WD will not show dramatic changes in the 1984-1986 period.
- 2) The OI 1305 resonance line is most probably blended with an upper ionization level line because its behaviour is similar to that of high level lines. The OI line is most probably emitted from a different nebula with conditions close to those of the ISM.
- 3) the systematic decrease and increase of the CII 1336 line, whose trend is opposite to that of the high ionization lines, indicates that the CII minimum is strongly correlated with the trend of the physical parameters, e.g. the ionization parameter, and the shock velocity. The role of the WD temperature is less prominent.

2.1. The UV-optical line spectrum at July 11 1986

FC95 in their table 3 report an optical spectrum in July 1986, observed at the same epoch as the UV spectrum presented in their table 2B, row 34.

We start by modeling the UV-optical combined spectrum observed at 11 July 1986 which is constrained by a relatively large number of lines from various ionization levels. This reveals the physical conditions in the emitting nebulae at that time. Such conditions will be adopted as a first guess in the modeling of the UV spectra in the next epochs.

The optical - UV spectrum at July 11 1986 is presented in Table 1. The lines are normalized to $H\beta = 1$.

Table 1: The UV and optical line ratios to $H\beta$ (July 11 1986)

line	obs	m_{34*}	m_{34}	line	obs	m_{34*}	m_{34}
NV 1240	3.7	55.	4.4	MgII 2800	+	-	-
OI 1306	0.74	0.77	0.01	[NeV] 3425	0.2	0.3	0.15
CII 1336	-	-	-	[NeIII] 3869	0.1	0.25	0.04
OV 1370	0.18	95.	0.3	$H\gamma$ 4360	0.31	0.38	0.4
SiIV] 1400	1.8	42.	1.6	[OIII] 4363	0.04	0.6	0.03
NIV] 1486	0.9	6.3	1.1	HeI 4471	0.087	0.005	0.024
CIV 1550	+	-	-	HeII 4686	0.6	0.6	0.67
HeII 1640	+	-	-	HeII 4686	0.6	0.6	0.67
OIII] 1643	1.0	29.	0.33	$H\beta$ 4861	1.	1.	1.
NIII] 1750	0.4	30.	0.2	HeI 5876	0.157	0.135	0.08
SiIII] 1890	0.5	28.	0.7	[FeVII] 6087	0.11	0.16	0.04
CIII] 1910	0.8	48.	1.1	$H\alpha$	6.2	5.6	3.1

Table 1 shows that the [OIII] 4363 line is not negligible, while the [OIII] 5007+4959 lines which are generally the strongest ones were not observed. This indicates a very high pre-shock density ($\sim 10^{8-9} \text{ cm}^{-3}$) characteristic of nebulae in SS (Angeloni et al. 2010).

The line intensities were reddening corrected adopting $E(B-V)=0.35$. Before correction $H\alpha / H\beta = 9.3$, after correction $H\alpha / H\beta = 6.2$ is still high compared to ~ 3 which results in the optically thin case (case A, Osterbrock 1989). Only in case A the lines with a relatively low critical density for collisional deexcitation (e.g. [OIII] 4363) can be observed. A higher $E(B-V)$ would result in abnormally high far UV line fluxes. Moreover, the observations in the IR do not suggest a large obscuration.

High $H\alpha / H\beta$ line ratios are typical of symbiotic stars. They could be due to radiative transfer effects of HI, to collision excitation of H lines, and, more specifically for symbiotic stars, to the effect of the viewing angle of the system (Contini 2003). In the following, we will consider the UV spectra independently from the $H\alpha / H\beta$ question.

Modeling the optical-UV spectrum, we have first fitted the ratios of the nitrogen lines, because N appears in three ionization levels (III, IV, and V), then we have considered the [NeV] and [NeIII] lines. The HeII lines depend strongly on the photoionization flux. The OV, SiIV], and SIV lines

are blended with the OIV] multiplet. The OI 1305 line is most probably blended with the SiII 1263,1308 doublet.

Model m_{34*} (Table 1) shows $H\alpha / H\beta > 5$ and reproduces most of the observed optical lines, except [OIII] 4363/ $H\beta$ which is overpredicted by a factor of 10. The spectrum is obtained by interrupting the downstream region at a distance of $5 \cdot 10^8$ cm from the shock front. The input parameters are $T_* = 1.2 \cdot 10^5$ K, $U=0.1$, $V_s = 80 \text{ km s}^{-1}$, $n_0 = 10^8 \text{ cm}^{-3}$, $B_0 = 10^{-3}$ gauss, and solar abundances. The density throughout the whole emitting region downstream is $> 10^9 \text{ cm}^{-3}$.

Although the [NeV]/[NeIII] line ratio is acceptable, most of the UV line ratios to $H\beta$ are overpredicted by a factor > 10 . Even assuming that the lines in the UV are emitted from a region different from that emitting the optical spectra, recall that all the spectral contributions must be summed up, adopting the same relative weights (see Contini et al 2009b) for UV and optical lines. This can produce less fitting results. A different reddening correction cannot help in this case, because it would overestimate the [OIII] 4363 line in the optical range.

Recent results obtained by modeling the AG Dra spectra (Contini & Angeloni 2011) imply collision of the WD wind with the shells ejected from the red giant. The shells contain grain and molecular dust leading to the underabundance of C, N, O, Si and Mg in the downstream gas because these elements are trapped into dust grains and molecules. Ne is not adsorbed in grains due to its atomic structure. Fe is also present in the gaseous phase.

Sputtering is not effective at velocities as low as those calculated from the FWHM of the line profiles. Fragmentation of matter at the shock front produces dense clumps of gas and dust. Adopting C, N, O, and Si abundances lower than solar by a factor > 10 relative to H, as for AG Dra, (Contini & Angeloni 2011) would improve the fit of the Z And spectrum. However, there is no other evidence to justify this assumption. Errors in the observations and uncertainties of the atomic coefficients adopted in the calculations cannot yield such discrepancies. So we will start by modeling the UV line ratios with relative abundances close to the solar ones and we will check the validity of this hypothesis by the spectra observed in the UV.

The model best fitting most of the UV and optical observations at July 1986 (m₃₄) is presented in Table 2, last row.

2.2. UV spectra

The UV spectra observed by FC95 and presented in their table 2B were reddening corrected and are shown in Table 3. They correspond to the following dates : JD 2440000+ 4719 : 24/Apr/81 ; +5797: 06/Apr/84 ; +5864 : 12/Jun/84 ; +5948 : 04/Sept/84 ; +6233 : 16/Jan/85 ; +6283 : 05/Aug/85 ; +6353 : 14/Oct/85 ; +6374 : 04/Nov/85 ; +6402 : 02/Dec/85 ; +6436 : 05/Jan/86 ; +6462 : 31/Jan/86 ; +6623 : 11/Jul/86.

We selected the spectra observed between Apr 24 1981 and Jul 11 1986 with the maximum number of lines, i.e. with the least number of saturated (+) and/or not detected fluxes (-). The spectrum observed at Nov 19 1980 is poor in number of lines, so we adopt April 1981 as the start of the first peak.

The three nitrogen lines are relatively strong and the NIV] line is present in all the significant spectra observed in the different epochs. Therefore, we normalise the line ratios to the NIV] 1486 multiplet summed terms, avoiding the element abundance problem at least for N. CIV 1550 which is generally a strong line, is saturated in many spectra. Both C and Si can be locked into grains so C and Si lines are less adapted to lead the modeling process. We wonder why the OIV] 1394-1407 multiplet was not observed and we suggest that the OIV] lines are blended with OV 1370 and with SiIV 1400. The S lines are not reported by FC95.

The observed line ratios to NIV] 1486 are compared with calculated line ratios in Table 3. The row containing the data at each epoch is followed by that showing the spectrum calculated by the model indicated in the first column. We reproduce the line ratios within a factor of ~ 2 . The fit of the line spectra and of the continuum SED at different days are cross-checked (Sect. 3).

The models are presented in Table 2. They were all calculated adopting solar abundances ($\text{He}/\text{H}=0.1$, $\text{C}/\text{H}=3.3 \cdot 10^{-4}$, $\text{N}/\text{H}=9 \cdot 10^{-5}$, $\text{O}/\text{H}=6.6 \cdot 10^{-4}$, $\text{Ne}/\text{H}=10^{-4}$, $\text{Mg}/\text{H}=2.6 \cdot 10^{-5}$, $\text{Si}/\text{H}=3.3 \cdot 10^{-5}$, $\text{S}/\text{H}=1.6 \cdot 10^{-5}$, $\text{Ar}/\text{H}=6.3 \cdot 10^{-6}$, $\text{Fe}/\text{H}=3.2 \cdot 10^{-5}$, Nussbaumer et al. 1988), except models m_{22} , m_{23} , and m_{30} , where $\text{C}/\text{H}=2.3 \cdot 10^{-4}$. In the last two columns of Table 2 the calculated absolute flux of $\text{H}\beta$ and the $\text{H}\beta$ /NIV] line ratios would provide the absolute flux values for all the lines.

The spectra show relatively strong lines from high ionization levels (e.g. NV 1240) as well as strong neutral lines (e.g. OI 1305) at the same time, indicating that the lines are emitted by different nebulae, as it was found for

Table 2: The models

model	V_s (km s ⁻¹)	n_0 (cm ⁻³)	D (cm)	T_* (K)	U -	$H\beta$ (erg cm ⁻² s ⁻¹)	$H\beta$ /NIV] -
mm	150	5.e8	8.7e13	1.2e5	0.0025	8.7e6	2.e3
m ₁₃	120	4.e7	2.e14	1.3e15	3.	4.e5	1.
m ₁₅	140	3.e7	3.6e13	1.4e5	2.	7.7e5	1.73
m ₁₇	210	6.e8	3.e9	1.4e5	0.5	1.1e4	0.7
m ₂₀	210	6.e8	3.4e9	1.4e5	0.6	1.1e4	0.68
m ₂₂	300	4.e8	1.3e10	1.7e5	0.8	1.3e4	1.3
m ₂₃	300	2.e8	1.7e10	1.6e5	0.4	6200.	1.15
m ₂₄	150	5.e8	1.1e9	>1.5e5	0.2	6738.	0.55
m ₂₅	110	1.e8	1.9e9	1.3e5	0.01	384.	0.52
m ₂₆	160	6.e7	4.4e9	1.3e5	0.08	335.	0.45
m ₂₈	100	5.e7	9.e9	1.3e5	0.08	130.	0.18
m ₃₀	150	8.e7	6.4e9	1.3e5	0.2	974.	0.376
m ₃₄	100	7.e7	8.e14	1.2e5	1.7	5.9e5	1.1

e.g. H1-36, AG Dra, and BI Cru (Angeloni et al 2007, Contini & Angeloni 2011, Contini al. 2009c). For Z And, a single-nebula model (m₃₄) in July 1986 and in the other epochs explains most of the observed spectrum, except the OI 1305 line. Table 3 shows that the contribution of a shock dominated nebula (model mm) characterised by a very low ionization parameter and high pre-shock density improves drastically the OI 1305/NIV] fit. The elements which can be trapped into dust grains, Si, Mg and C, are depleted from the gaseous phase, while oxygen is only slightly depleted (Si/H= 3.3 10⁻⁶ Mg/H=2.610⁻⁸, C/H= 2. 10⁻⁴ and O/H=6. 10⁻⁴). This model also improves the modeling of other line ratios, such as SiIII] 1890 at Apr 1984, June 1984, Jan 1985, Aug 1985 and Oct 1985 if summed up to models m₁₃-m₃₄ adopting different weights.

Models m₁₃-m₃₄ represent the nebula downstream of the shock front propagating towards the WD, while model mm represents dusty clumps created by fragmentation of matter by collision with RG debris.

2.3. Results

The visual light curve (Fig. 1) covers a frequency band accounting for lines and continuum in the optical range. The strongest lines are generally

Table 3: Comparison of calculated with observed line ratios to NIV]=1

JD ¹	NV 1240	OI 1305	CII 1335	OV 1370	SiIV 1400	CIV 1550	HeII 1640	OIII] 1663	NIII 1750	SiIII] 1890	CIII] 1910	MgII 2800
4719	8.4	0.69	-	-	2	9.6	7.9	1.03	0.24	0.62	0.81	-
m ₁₃	7.7	-	-	-	1	8.7	7.1	0.34	0.2	1.4	1.8	-
5797	2.75	0.53	0.03	0.24	1.7	5.91	+	1.	0.55	0.66	0.7	+
m ₁₅	2.6	-	0.2	0.4	0.9	12.2	12.9	0.7	0.4	2.3	3.	-
5864	4.77	0.97	0.03	0.85	0.9	+	+	+	0.5	0.59	+	+
m ₁₇	4.7	0.05	0.24	0.43	3	-	5.3	1.2	0.5	6.3	-	-
5948	4.0	0.98	0.02	-	2.3	+	5.3	1.	0.4	0.54	0.59	0.09
m ₂₀	4.6	0.04	0.16	-	3.	-	5.2	1.	0.4	0.54	0.54	0.13
6233	8.8	0.17	0.04	0.4	3.6	+	8.28	0.97	0.33	0.43	0.7	+
m ₂₂	7.4	0.1	0.3	0.7	4.	-	9.8	1.58	0.6	10.	0.8	-
6283	5.87	1.	-	0.58	2.56	9.9	7.17	1.03	0.38	0.59	0.95	-
m ₂₃	5.3	0.1	-	0.5	2.2	1.6	7.7	2.7	1.	10.	1.7	-
6353	3.9	0.52	0.07	0.18	+	11.5	4.56	1.3	+	0.3	1.4	+
m ₂₄	3.	-	0.1	0.3	5.2	17.	4.0	1.47	-	5.	1.2	-
6374	1.17	1.1	0.24	-	4.85	14.	1.23	3.57	2.54	3.0	4.96	0.5
m ₂₅	1.2	0.1	2.6	-	4.5	14.	1.25	3.1	2.	3.6	5.2	2.4
6402	4.29	2.	0.5	-	5.68	11.3	1.35	3.88	2.65	4.16	5.06	+
m ₂₆	3.8	0.1	0.8	-	6.5	13.3	1.1	2.8	1.8	3.	4.	-
6436	0.87	1.48	0.63	-	4.19	7.	0.51	2.59	2.09	4.07	3.53	0.27
m ₂₈	1.	0.1	0.2	-	4.	11.	1.3	1.2	1.	2.	3.2	0.12
6462	0.8	1.51	-	-	4.16	5.63	1.53	2.16	1.78	+	+	0.14
m ₃₀	1.6	-	-	-	4.7	10.	2.6	1.6	1.	3.5	-	0.23
6623	4.03	0.8	-	0.2	2.26	+	+	1.09	0.46	0.48	0.84	+
m ₃₄	4.4	0.01	-	0.3	1.6	-	-	0.33	0.2	0.65	1.1	-
mm	4.6	1.1	5.	1.	3.	10.4	0.8	2.6	0.8	0.49	1.1	3.2

¹ 2440000+

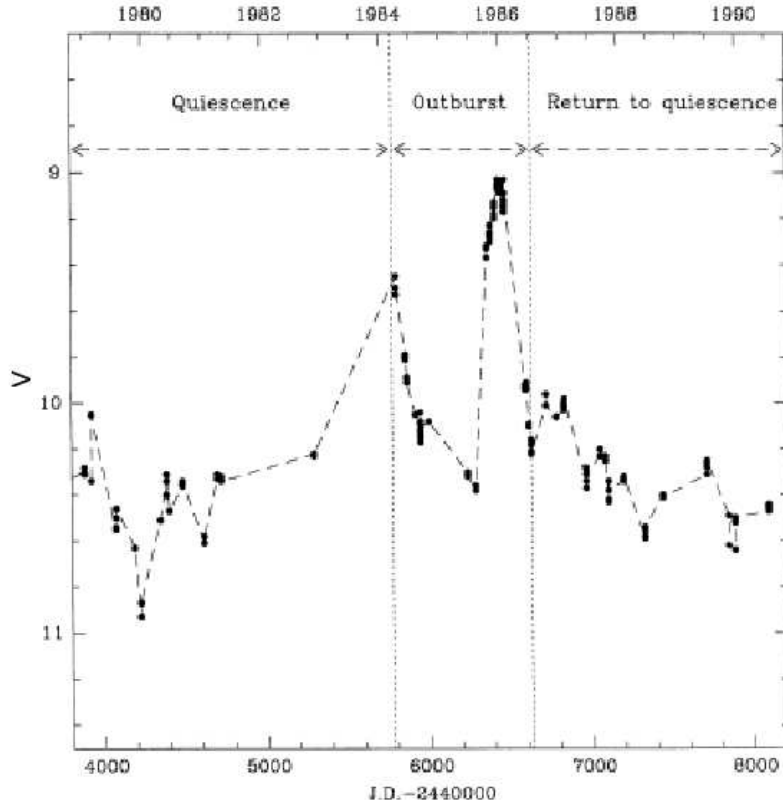


Figure 1: Top : the FES light curve of Z And adapted from FC95 (fig 1). Dotted black lines define the outburst.

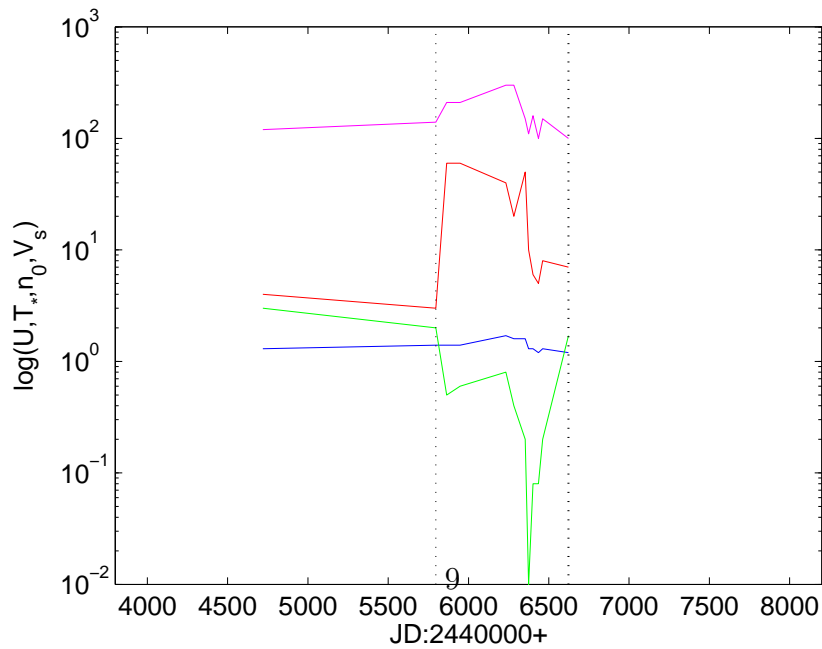


Figure 2: The physical parameters (in logarithm scale) across the outburst calculated by modeling the line spectra. V_s : magenta; n_0 (in units of 10^7 cm^{-3}) : red; T_* (in units of 10^5 K) : blue ; U : green. Dotted black lines define the outburst.

HeII 4686, $H\beta$, [OIII]5007, 4959, etc., while the optical spectrum (FC95) shows relatively low forbidden lines. So we consider that the main contributors to the visual band are HeII 4686 and $H\beta$, which depend strongly on the WD temperature and on the ionization parameter. T_* and U affect the spectra in the same way. Namely, when they decrease, the high level lines decrease relatively to the low level ones.

The increase of T_* at the epochs of the peaks and the decrease at minima would indicate that the active phase is characterised by two different bursts. On the other hand, if T_* does not change significantly and only U changes, a disturbing dynamical and/or morphological event between the radiation source and the nebula is most likely the source of the visual curve minimum.

The UV band accounts for lines from different levels which are variously modified by T_* and U fluctuation. Moreover, the shock velocity and the compression downstream affect the stratification of the ions and, consequently, the line ratios. FC95 show that lines from different ionization levels have different trends throughout the 1984-1986 time period. We predict that the UV light curve throughout the outburst, would have a profile different from that reported in Fig. 1.

In Fig. 2 we present the physical parameters obtained by modeling the spectra throughout the 1984-1986 outburst. The profiles of the physical conditions are rather unexpected if compared with the visual light curve (Fig. 1).

The sudden increase of the density on April 1984, accompanied by the sudden increase of the velocity, indicates that collision of the WD wind with a shell ejected from the red giant is occurring. The nebula downstream of the reverse shock is heated and ionized by both the shock and the photoionization flux from the hot star. In the next days the density and the shock velocity have opposite trends in agreement with conservation of mass at the shock front ($n_1 v_1 = n_0 v_0$, from the Rankine-Hugoniot equations). In the meanwhile the temperature of the hot star is slightly increasing from $\sim 120,000$ K to a maximum of $170,000$ K, corresponding to the outburst maximum, in agreement with FC95. The drop of U on 1984 toward July 1986 shows that the spectra during that epoch are dominated by a relatively strong shock, i.e. the reverse shock, which vanishes at a certain time, depending on the outburst characteristics (Chevalier 1982).

The second density peak at December 1985-January 1986 reveals that collision of the WD wind with another RG shell has occurred. The ionization parameter drop by more than two orders of magnitude after June

1985, accompanied by the simultaneous variation of the dynamical parameters V_s and n_0 , suggests that the shock front has suddenly shifted farther from the WD.

The matter downstream of the reverse shock front is fragmented by Richtmyer-Meshkov and Kelvin-Helmholtz instabilities. High density fragments between the stars eventually prevent the black body flux from reaching the nebula. However, the decline of the BB flux by fragment obstruction could indeed reduce the ionization parameter, but less sharply than predicted by the calculations. So, the whole picture is most likely explained by an unexpected disturbing episode such as the ejection of a new shell from the RG atmosphere and its collision with the WD wind at a relatively large distance from the WD (Sect. 3).

The gas composition at the epochs of collision with the shells reveals that the calculated SiIII]/NIV] line ratios would better reproduce the data adopting Si/H relative abundances lower than solar by a factor of 4 for models m_{13} , m_{15} and of ~ 10 for models m_{17} , m_{22} , m_{23} , m_{24} . This indicates that silicate grains are present after collision of the WD wind with the first RG shell. On the other hand Si is in the gaseous phase with a solar Si/H relative abundance at the epochs corresponding to models m_{26} , m_{28} , m_{30} , m_{34} . The grains had not enough time to form at collision with the next shell. Grain formation time scales (Gail et al 1984, Scalo & Slavsky 1980) are as long as ~ 1 year. However, in circumstellar shells the chemical equilibrium and consequently grain formation is disturbed by the UV radiation from the WD and by the velocity field (Gail et al. 1987).

3. The continuum

In Fig. 3 we compare the observed continuum SED with model calculations.

3.1. The continuum SED

We refer to the SED of the continuum flux presented by FC95 in their fig. 8. We have used the data in the UV and in the radio range presented by FC95 tables 2A and 4, respectively. The dates corresponding to observations in the radio and those in the other frequency ranges are not exactly coincident, e.g. we adapted the radio fluxes observed in October 1986 to data observed in July 1986.

Each diagram of Fig. 3 presents the free-free + free-bound fluxes emitted from the nebula at a certain epoch. They are calculated by the same models (Table 2) which lead to the best fit of the line spectrum (Table 3). Moreover, the BB flux from the RG corresponding to a temperature of 3200 K (FC95), and the BB flux corresponding to the WD which was derived by modeling the line spectrum are also shown. Reprocessed radiation of dust within the nebula calculated consistently with gas emission is added in Fig. 3 diagrams. This flux is mostly hidden by the BB flux from the RG if dust-to-gas ratios of 10^{-14} by number ($4 \cdot 10^{-4}$ by mass for silicates) are adopted. Actually, the dust-to-gas ratios are constrained by the data in the mid-IR.

Fig. 3 shows that the emission from the nebula appears in a small frequency range between the optical and the near-UV ($\sim 1\text{--}3 \cdot 10^{15}$ Hz), depending on the epoch. There are no data in the soft X-ray range and beyond it. We can predict that bremsstrahlung from the nebula downstream of shock fronts with $V_s \geq 160 \text{ km s}^{-1}$ would be the X-ray source. For lower velocities the SED in the soft X-ray range is the summed flux of bremsstrahlung from the nebulae and BB flux from the WD. The contribution to soft-X-rays up to the X-ray domain of bremsstrahlung from shocked nebulae was suggested for the symbiotic system AG Dra by Contini & Angeloni (2011).

The fit of calculated to observed data is good enough to confirm a strong self-absorption of free-free radiation from the nebulae for frequencies $< 10^{13}$ Hz.

Finally, Fig. 3 diagrams show that the BB flux from the RG and from the nebula dominate the SED in the visual, while the flux from the WD appear in the UV and soft X-ray range. This indicates that strong variations in the WD temperature that generally accompany the outbursts cannot be directly revealed by the visual light curve presented by FC95, but only indirectly by the spectra emitted from the nebula.

3.2. Radius of the nebulae

In previous works on SS, e.g. CH Cyg (Contini et al 2009b), AG Dra (Contini & Angeloni 2011), etc. we calculated the distance r of the nebulae from the center of the SS adjusting the continuum fluxes calculated by the models at the nebula to those observed at Earth. We defined the adjusting factor η by $r^2 = 10^{-\eta} d^2 ff$, where ff is the filling factor and d the distance to Earth.

Adopting a distance of Z And to Earth of 1.12 kpc (Viotti 1982), the best fit to the data of the bremsstrahlung calculated from the nebulae downstream

of the shock front, gives $r = 1.9 \cdot 10^{14}$ cm at April 1981, $r = 1.4 \cdot 10^{14}$ cm at April 1984, $r = 9.4 \cdot 10^{15}$ cm at December 1985, and $r = 2.7 \cdot 10^{14}$ cm at July 1986. The distances were calculated by a filling factor $\mathcal{f} = 1$.

Considering that : $F_\nu (R_{WD}/r)^2 = U n c$ (where F_ν is the flux from the WD, R_{WD} is the radius of the WD, n is the density of the gas and c the speed of light), the results suggest that the drop of the ionization parameter U between November and December 1985 most probably derives from the sudden increase of the distance from the hot source. This is explained by the ejection of the next shell in the RG atmosphere.

The collision between the wind from the WD and the two shells from the RG occurred within less than 2 years, from March 1984 to November 1985. The shock front has therefore expanded from $\sim 2 \cdot 10^{14}$ to $\sim 9 \cdot 10^{15}$ cm, by an average velocity of $\sim 130 \text{ km s}^{-1}$, in rough agreement with the observations.

4. Discussion and concluding remarks

The 1984-1986 outburst of Z And is revisited by a detailed modeling of the spectra. Comparing the visual light curve of Z And during the 1984-1986 outburst with those in other epochs from 1895 up to 2007 September, the 1984-1986 event is remarkable for its double peaked structure and for its low brightness.

We explain the burst double structure in the light of red giant pulsation, by the collision of the WD wind with two ejected shells. The minimum of the light curve between the two peaks is accompanied by the dip of the ionization parameter which is constrained by the detailed modeling the UV line spectra at November-December 1985. The sharp drop of U is due to the sudden increase of the distance between the WD and the downstream nebula reached by the WD black body flux, namely, the collision of the WD wind with a new shell in the RG atmosphere. Since the shell was recently formed at the time of observations, the grains did not have enough time to develop. This is revealed by the solar relative abundance of Si/H.

We suggest that the outburst did not attain its maximum luminosity because the collision of the wind network was distorted by the oncoming of the next shell.

The small peaks in the light curve before and after the 1984-1986 burst are most probably due to RG shell ejections. The periodicity of the maxima is in fact of ~ 300 -400 days.

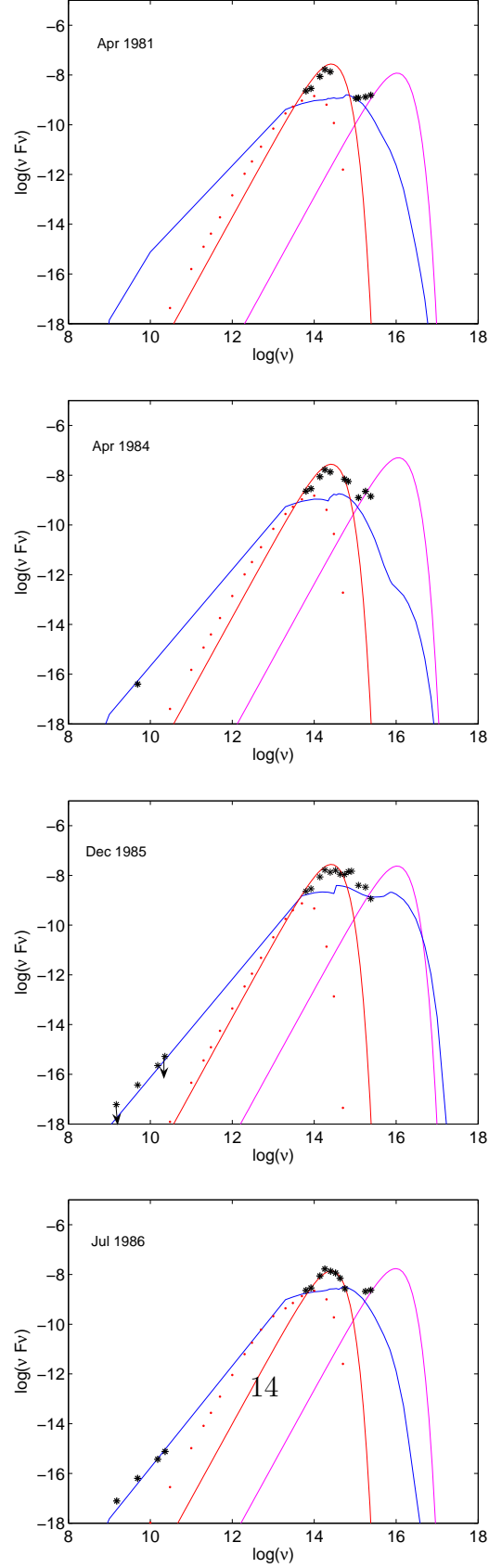


Figure 3: The continuum SED in the different epochs. Red giant bb flux ($T=3200$ K)

During the 2000-2002 outburst of Z And, broad wings (up to 2000 km s^{-1}) developed in the $\text{H}\alpha$ line profile (Tomov et al 2008). Moreover, collimated bipolar jets appeared and disappeared throughout the 2006 outburst (Skopal et al 2009). Broad lines were observed in other SS, e.g. CH Cyg, BI Cru, AG Dra, etc. They originate from the high velocity matter accompanying the outbursts. Exceptionally broad $\text{Ly}\alpha$ and $\text{H}\alpha$ line profiles were explained by WD explosion (Contini et al. 2009 a,c), while collimated jets at some epochs reveal the presence of the accretion disk. Both broad lines and jets were not observed during the 1984-1986 outburst of Z And.

Acknowledgments

We are grateful to Sharon Sadeh for helpful advise.

References

- [1] Angeloni, R., Contini, M., Ciroi, S., Rafanelli, P. 2007, A&A, 471, 825
- [2] Angeloni, R., Contini, M., Ciroi, S., Rafanelli, P. 2010, MNRAS, 402, 207
- [3] Bisikalo, D.V., Boyarchuk, A.A., Kilpio, E. Yu, Tomov, N.A., Tomova, M.T. 2006, Astron. Rep., 50, 722
- [4] Chevalier, R.A., 1982, ApJ, 259, L85
- [5] Contini, M. 2003, MNRAS, 339, 125
- [6] Contini, M., Angeloni, R., 2011 New Astr., 16, 199
- [7] Contini, M., Angeloni, R., Rafanelli, P. 2009a, A&A, 496, 759
- [8] Contini, M., Angeloni, R., Rafanelli, P. 2009b, AN, 330, 816
- [9] Contini, M., Angeloni, R., Rafanelli, P. 2009c, MNRAS, 396, 807
- [10] Fernández-Castro, T., González-Riestra, R., Cassatella, A., Taylor, A.R., Seaquist, E.R. ApJ, 1995, 442, 366
- [11] Gail, H.-P.; Keller, R.; Sedlmayr, E. 1984, A&A, 133, 320

- [12] Gail, H.-P., Gauger, A.; Goeres, A.; Henkel, R.; Sedlmayr, E. 1987, MitAG, 70, 365
- [13] Girard, T., Willson, L.A., 1987, A&A, 183,247
- [14] Kenyon, S.J., Webbink, R.F. 1984, ApJ, 279, 252
- [15] Leibowitz, E. M.; Formigini, L. 2008 MNRAS. 385, 445
- [16] Nussbaumer, H., Schild, H., Schmid, H.M., Vogel, M. 1988, A&A, 198, 179
- [17] Osterbrock, D.E. 1988 in 'Astrophysics of gaseous nebulae and active galactic nuclei', University Science Books
- [18] Scalo, J.M., Slavsky, D.B. 1980, ApJ, 239, L73
- [19] Saquist, E.R., Taylor, A.R., Button, S. 1984, ApJ, 284, 202
- [20] Skopal, A. et al. 2009, ApJ, 690, 1222
- [21] Sokoloski, J.L. et al. 2006 ApJ, 636, 1002
- [22] Tomov, N.A., Tomova, M.T., Bisikalo, D.V. 2008 MNRAS, 389, 829
- [23] Viotti, R., Giangrande, A., Ricciardi, O., Cassatella, A. 1982 in 'The Nature of Symbiotic Stars', ed. M. Friedjung and R. Viotti (Dordrecht:Reidel), 125